

Binding interactions control SNARE specificity in vivo

Hui-Ju Yang,¹ Hideki Nakanishi,¹ Song Liu,² James A. McNew,² and Aaron M. Neiman¹

¹Department of Biochemistry and Cell Biology, Stony Brook University, Stony Brook, NY 11794

²Department of Biochemistry and Cell Biology, Rice University, Houston, TX 77251

S*accharomyces cerevisiae* contains two SNAP25 paralogues, Sec9 and Spo20, which mediate vesicle fusion at the plasma membrane and the prospore membrane, respectively. Fusion at the prospore membrane is sensitive to perturbation of the central ionic layer of the SNARE complex. Mutation of the central glutamine of the t-SNARE Sso1 impaired sporulation, but does not affect vegetative growth. Suppression of the sporulation defect of an *sso1* mutant requires expression of a chimeric form of Spo20 carrying the SNARE helices

of Sec9. Mutation of two residues in one SNARE domain of Spo20 to match those in Sec9 created a form of Spo20 that restores sporulation in the presence of the *sso1* mutant and can replace *SEC9* in vegetative cells. This mutant form of Spo20 displayed enhanced activity in in vitro fusion assays, as well as tighter binding to Sso1 and Snc2. These results demonstrate that differences within the SNARE helices can discriminate between closely related SNAREs for function in vivo.

Introduction

Control of membrane fusion events is critical for the maintenance of an organized endomembrane system in eukaryotic cells. Fusion must be regulated so that carrier vesicles only fuse with the appropriate acceptor compartment. This control is exerted on several levels by a variety of regulatory proteins including SM proteins, Rab proteins, and tethering complexes (McNew, 2008). Additionally, specific interactions between SNARE proteins are an important factor in the specificity of vesicle fusion (Sollner et al., 1993; McNew et al., 2000).

SNARE proteins are the core machinery of intracellular membrane fusion (Weber et al., 1998). They are characterized by a ~60 amino acid domain (the SNARE domain) through which they form heterooligomers (Sutton et al., 1998; Weimbs et al., 1998). In addition, most SNARE proteins contain a C-terminal transmembrane domain adjacent to the SNARE domain. Interaction of a SNARE protein anchored in the vesicle membrane (a v-SNARE) with SNARE proteins in the target membrane (t-SNAREs) leads to the assembly of the SNARE domains into a parallel four-helix bundle (Poirier et al., 1998; Sutton et al., 1998). Bundle formation drives the transmembrane domains of the SNAREs into close proximity and is proposed to provide the

potential energy necessary to allow mixing and fusion of the lipid bilayers (Weber et al., 1998; Jahn and Scheller, 2006).

Discrete SNARE complexes control fusion at every level of the secretory pathway (Pelham, 1999). This has led to the suggestion that assembly of cognate SNAREs into exclusive complexes could be a central mechanism for the control of vesicle fusion in the cell (Sollner et al., 1993; McNew et al., 2000). Though isolated SNARE domains show little or no binding specificity in vitro, when full-length SNAREs are reconstituted into synthetic liposomes, only specific combinations can mediate fusion of the artificial bilayers, suggesting that this could be the basis for in vivo control (Yang et al., 1999; McNew et al., 2000). However, many SNAREs have been found to participate in more than one fusion event in vivo and in vitro (Parlati et al., 2000, 2002; Paumet et al., 2001, 2004), again raising the question of how the participation of an individual SNARE in a particular fusion event is regulated.

The process of sporulation in the budding yeast *Saccharomyces cerevisiae* provides a useful model in which to address the question of SNARE specificity. During sporulation, fusion of post-Golgi vesicles with the plasma membrane stops, and instead these vesicles are directed to specific sites in the cytoplasm

Correspondence to Aaron Neiman: Aaron.Neiman@sunysb.edu

H. Nakanishi's present address is Department of Cell Science, Institute of Biomedical Sciences, Fukushima Medical University School of Medicine, Fukushima 960-1295, Japan.

Abbreviation used in this paper: 5-FOA, 5-fluoroorotic acid.

© 2008 Yang et al. This article is distributed under the terms of an Attribution-Noncommercial-Share Alike-No Mirror Sites license for the first six months after the publication date [see <http://www.jcb.org/misc/terms.shtml>]. After six months it is available under a Creative Commons License [Attribution-Noncommercial-Share Alike 3.0 Unported license, as described at <http://creativecommons.org/licenses/by-nc-sa/3.0/>].

where they fuse to form new membrane compartments termed prospore membranes (Neiman, 1998). One prospore membrane envelops each of the four nuclei produced by meiosis, packaging the nuclei into four daughter cells or spores (Neiman, 2005). In concert with this change in the target compartment of exocytic vesicles comes a change in one of the SNARE proteins required for their fusion (Neiman, 1998).

In vegetative cells, vesicles fusing with the plasma membrane use a SNARE complex that is composed of one of two redundant t-SNAREs Sso1 or Sso2, a second t-SNARE subunit, Sec9, and one of two redundant v-SNARE proteins Snc1 or Snc2 (Aalto et al., 1993; Protopopov et al., 1993; Brennwald et al., 1994). Sec9 is a member of the SNAP25 subfamily of SNARE proteins, which differ from other SNAREs in that they lack a transmembrane domain but contain two SNARE helices (Oyler et al., 1989; Brennwald et al., 1994; Weimbs et al., 1998). Thus, a SNARE complex acting at the plasma membrane contains one helix from Sso1 or Sso2, one helix from Snc1 or Snc2, and two helices from Sec9. During sporulation, when exocytic vesicles fuse to generate a prospore membrane, the SNARE complex used is slightly different. Sso1 is required for this fusion, but Sso2 does not function in this process (Jantti et al., 2002). An *ssol* single mutant, though normal for vegetative secretion, is completely blocked in fusion during sporulation. Direct evidence that Snc1 or Snc2 function at the prospore membrane has not been reported, but a role for these v-SNAREs has been inferred by their localization to the prospore membrane during sporulation (Neiman et al., 2000). Finally, the most notable difference is that the t-SNARE Sec9 is not required for fusion at the prospore membrane. Rather, it is replaced by a second sporulation-specific SNAP25 family member, the Spo20 protein (Neiman, 1998).

Sec9 and Spo20 are specialized for their sites of action. Ectopic expression of *SPO20* in vegetative cells cannot rescue the growth defect of a *sec9-4^{ts}* mutant at 37°C, nor can overexpression of *SEC9* during sporulation restore sporulation to a *spo20* mutant (Neiman, 1998). Chimera studies indicated that the basis of specificity is different for each protein. The ability of Spo20 to work at the prospore membrane requires a lipid-binding motif in its N-terminal domain that is not present in Sec9 (Neiman, 1998; Nakanishi et al., 2004). Targeting of Sec9 to the prospore membrane allows it to largely compensate for loss of *SPO20* (Nakanishi et al., 2006). In contrast, the ability of Sec9 to function at the plasma membrane is a property of its SNARE domains. Forms of Spo20 in which the SNARE domains are substituted with those of Sec9 can replace *SEC9* in vegetative cells (Neiman et al., 2000). Changes in genes involved in lipid metabolism were also found to promote the function of Spo20 in vegetative cells (Coluccio et al., 2004). Finally, in vitro experiments comparing Sso1/Sec9–Snc2 and Sso1/Spo20–Snc2 complexes demonstrated that the Spo20-containing assemblies are less potent fusogens and that the stability of the assembled complexes is lower (Liu et al., 2007). These results suggest that the inability of Spo20 to function at the plasma membrane may be a function of it forming complexes that provide insufficient binding energy to overcome a barrier to fusion at that compartment.

An assembled SNARE complex incorporates sixteen interfaces where the side chains from all four helices pack to-

gether (Sutton et al., 1998). The packing interactions are primarily hydrophobic contacts, except at the central or “zero layer” interface (Sutton et al., 1998). There, the interaction is mediated by polar binding between conserved glutamine and arginine side chains. Most SNARE complexes conform to a 3Q:1R rule, i.e., at the zero layer, three glutamine residues interact with one arginine (Fasshauer et al., 1998). In the yeast plasma membrane SNARE, Sso1/Sso2 and both helices from Sec9 contain a glutamine residue, and Snc1/Snc2 provides the arginine residue. If the central layer glutamine in Sso1 is mutated to arginine, this mutant form of Sso1 is not functional; however, function can be restored by coexpression of a form of Snc2 in which the arginine has been changed to glutamine (Katz and Brennwald, 2000). Such compensatory Q/R mutations also work in other SNARE complexes and have been used to demonstrate that specific pairs of SNARE proteins function together in vivo (Graf et al., 2005).

The interpretation of the Spo20 experiments described above assumes that the Snc1/Snc2 proteins function as the v-SNARE for fusion at the prospore membrane. To test this, we sought to use compensatory Q/R mutations in the SNARE domains of Sso1 and Snc2 to demonstrate a direct role of Snc2 during sporulation. We report here that strains carrying an Sso1^{Q224R} mutation failed to sporulate, and that compensatory mutations in none of the *S. cerevisiae* R-SNAREs can rescue this sporulation defect. Sporulation is reduced by mutation of the central layer glutamine of Sso1 to any other residue, whereas vegetative growth is largely unaffected by these changes. The sensitivity of sporulation to changes in the Sso1 ionic layer residue, we show, is due to the presence of Spo20 in the prospore membrane SNARE complex. Co-expression of a Spo20 chimera carrying the Sec9 SNARE helices with the Snc2^{R52Q} allele rescues the sporulation defect of the *ssol*^{Q224R} mutant. Mutation of two residues located at binding interfaces in the SNARE domain of Spo20 to the corresponding residue in Sec9 allows Spo20 to function in concert with Sso1^{Q224R} and Snc2^{R52Q} proteins. This mutant form of Spo20 also shows enhanced ability to rescue *sec9-4^{ts}* in vegetative cells. In vitro, the mutant Spo20 forms tighter complexes with Sso1 and Snc2 and is a more efficient fusogen than the wild-type protein. These results demonstrate that the intrinsic binding energy of the SNARE domains can help control the specificity of vesicle fusion in vivo.

Results

Compensatory mutations in Snc2 cannot rescue the sporulation defect of a mutation in the Sso1 central ionic layer

Prospore membrane formation requires the t-SNAREs Sso1p and Spo20p (Neiman, 1998; Jantti et al., 2002). Though the v-SNAREs Snc1p and Snc2p localize to the prospore membrane (Neiman et al., 2000), direct evidence of their involvement in prospore membrane assembly has not been reported. Compensatory Q/R mutations in the central ionic layer of a t-SNARE and a v-SNARE have been used to demonstrate specific SNARE interactions in vivo (Katz and Brennwald, 2000; Graf et al., 2005). To examine the possible role of the Snc proteins during sporulation, we introduced a plasmid carrying the *ssol*^{Q224R} allele into strain HI3 (*ssol/ssol*) alone or in combination with a


Relevant Genotype	Gene expressed	% asci	Ether test
<i>sso1ΔSSO2</i>	none	< 0.2	
<i>sso1ΔSSO2</i>	<i>SSO1</i>	40.4	
<i>sso1ΔSSO2</i>	<i>sso1</i> ^{Q224R}	< 0.2	
<i>sso1ΔSSO2</i>	<i>sso1</i> ^{Q224R} <i>snc2</i> ^{R52Q}	< 0.2	
<i>sso1Δsso2Δ</i>	<i>sso1</i> ^{Q224R} <i>snc2</i> ^{R52Q}	< 0.2	

Figure 1. **Compensatory mutation of *SNC2* cannot rescue the sporulation defect of *sso1*^{Q224R}.** Strains HI3 (*sso1Δ/sso1Δ*) or HI75 (*sso1Δ/sso1Δ sso2Δ/sso2Δ*) were transformed with the CEN plasmids expressing the indicated genes and sporulated in liquid culture. Sporulation was assessed by observation in the light microscope and by ether test. To determine percentage of sporulation, at least 500 cells were counted for each strain. For HI75, the plasmid carrying the wild-type *SSO1* was lost by growth on 5-FOA before cells were assayed.

plasmid carrying the *snc2*^{R52Q} allele. As expected, the *sso1*^{Q224R} allele did not rescue the sporulation defect of the *sso1Δ* (Fig. 1). Neither *SNC2* nor *snc2*^{R52Q} were capable of restoring sporulation in this context (Fig. 1). This failure of *snc2*^{R52Q} to rescue the sporulation defect raises the possibility that Snc2p does not participate in vesicle fusion at the prospore membrane. We therefore examined whether mutation of the central layer arginine to glutamine in any of the other *S. cerevisiae* R-SNAREs (Snc1, Ykt6, Sec22, Nyv1) could restore sporulation to the *sso1*^{Q224R} strain. As with *snc2*^{R52Q}, none of these mutant SNAREs could compensate for the *sso1*^{Q224R} mutation (unpublished data).

To ensure that *snc2*^{R52Q} was indeed capable of suppressing *sso1*^{Q224R} in our strains, we constructed a strain homozygous for deletion of *SSO1* and *SSO2* and kept alive by the *SSO1* gene on a centromeric plasmid (HI75). When the *sso1*^{Q224R} mutation was introduced into this strain, the plasmid bearing the wild-type gene could be lost only when the *snc2*^{R52Q} allele was also present. The resulting strain is viable because of the compensatory interaction between the two mutant SNAREs (Katz and Brennwald, 2000). However, as with the results in the *sso1Δ/sso1Δ* strain, the presence of *snc2*^{R52Q} does not rescue the sporulation

defect associated with *sso1*^{Q224R} (Fig. 1). Together, these results suggest either that no R-SNARE proteins are involved in fusion at the prospore membrane, and therefore they cannot compensate for the *sso1*^{Q224R} mutation, or that fusion at the prospore membrane is particularly sensitive to the proper configuration of side chains at the central ionic layer in the SNARE complex.

Vegetative yeast cells are largely insensitive to mutation of the t-SNARE ionic layer

To further explore the role of the central ionic layer in Sso1 function, codon 224 was mutated and alleles bearing all possible amino acid replacements of the glutamine were constructed. Each of these *sso1*^{Q224X} alleles was introduced on a plasmid into strain HI75 (*sso1Δ/sso1Δ sso2Δ/sso2Δ pSSO1*) and the transformants were then transferred to plates containing 5-fluoro-orotic acid (5-FOA) to select for loss of the wild-type *SSO1*-containing plasmid. Like *sso1*^{Q224R}, *sso1*^{Q224P} failed to grow on 5-FOA, indicating that a proline substitution at this position also interferes with Sso1 function. Though arginine cannot function, lysine is weakly tolerated at this position as cells containing *sso1*^{Q224K} as their only source of Sso protein were viable, but slow growing at elevated temperature (Fig. 2). The phenotype of *sso1*^{Q224K} may be due to the presence of the positively charged side chain because, as with *sso1*^{Q224R}, coexpression of *snc2*^{R52Q} suppressed the slow growth of *sso1*^{Q224K} (unpublished data). However, other than these three mutations, all other amino acids at position 224 were well tolerated. As judged by colony size, strains carrying these *sso1*^{Q224X} alleles as their sole form *SSO* grew as well as those carrying *SSO1* even at low or high temperatures (Fig. 2; not depicted). Thus, despite the strong evolutionary conservation of ionic layer glutamine, the yeast plasma membrane SNARE can tolerate a wide variety of residues at this position.

Sporulation is sensitive to perturbation of Sso1^{Q224}

The strains carrying the various *sso1*^{Q224X} alleles as their only *SSO* were then examined for their ability to sporulate. Unlike growth rate, sporulation was sensitive to changes at this position (Fig. 3).

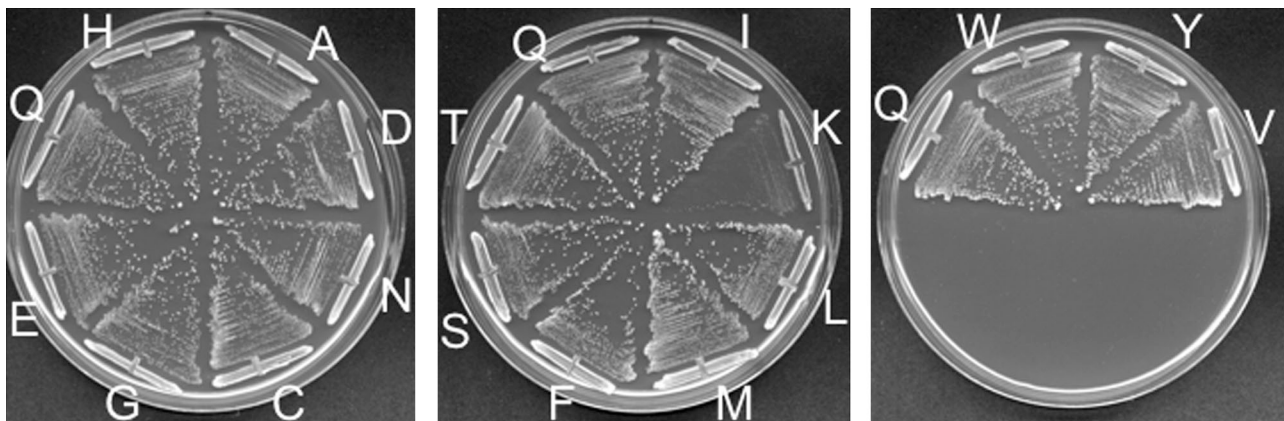


Figure 2. **Mutation of Sso1^{Q224} is well tolerated in vegetative growth.** Strain HI75 (*sso1Δ/sso1Δ sso2Δ/sso2Δ*) was transformed with CEN plasmids carrying all possible amino acid substitutions at position 224 of Sso1 and the plasmid carrying the wild-type *SSO1* was lost by plasmid shuffle, leaving the mutant as the sole form of Sso protein in the cell. Transformants carrying substitutions that could support growth (all except arginine and proline) were streaked out on YPD plates and incubated at 37°C. Letters indicate the amino acid present at position 224 of Sso1 in each strain.

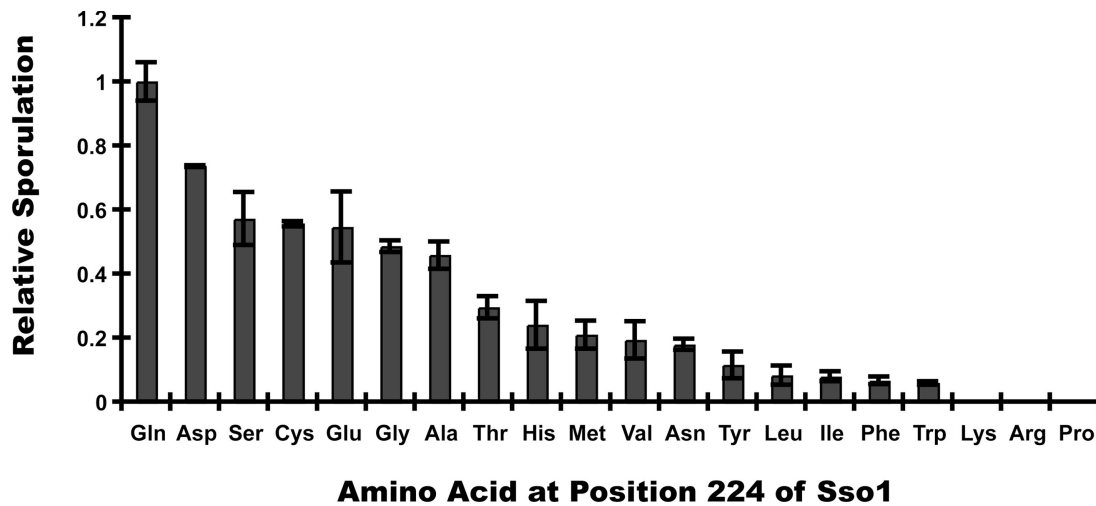


Figure 3. **Sporulation is sensitive to mutation of Sso1Q224.** Strains HI3 (*sso1Δ/sso1Δ*) (for Sso1Q224R, Q224P, and Q224K) or HI75 (*sso1Δ/sso1Δ sso2Δ/sso2Δ*) (all other substitutions) expressing an *SSO1* gene with the indicated amino acid substitution from a CEN plasmid were sporulated, and the percentage of sporulation in the culture was measured. At least 500 cells were counted for each strain. Sporulation efficiency is shown relative to HI75 carrying the wild-type *SSO1*. Error bars indicate one standard deviation.

All of the mutations caused a reduction in sporulation efficiency, varying from a two- to fourfold to several hundredfold with small or polar amino acids better tolerated than large hydrophobic or positively charged side chains. Substitution of glutamine 224 to lysine, which causes slow vegetative growth, led to a complete loss of sporulation, as did the arginine and proline mutations (examined in the *sso1* single mutant strain) that cannot support vegetative growth. Substitution to leucine or tryptophan had no effect on growth rate, yet these mutants displayed strong sporulation defects. Thus, mutations such as *sso1*^{Q224W} behave as sporulation-specific alleles of *SSO1*; they are as effective as wild-type in supporting vegetative growth but poorly support sporulation. These results suggest that the inability of *snc2*^{R52Q} to rescue the sporulation defect of *sso1*^{Q224R} might be caused by the sensitivity of sporulation to changes in the ionic layer residue of Sso1, rather than an indication that Snc2 does not function at the prospore membrane.

The combination of Snc2^{R52Q} and Sec9 helices can rescue the sporulation defect of *sso1*^{Q224R}

One possible explanation for the observation that *snc2*^{R52Q} can only rescue *sso1*^{Q224R} during vegetative growth is that one or both of these mutant proteins is mislocalized during sporulation. However, examination of GFP-tagged forms of the proteins revealed that both display an SPB-associated fluorescence in *sso1* mutant cells indistinguishable from wild-type Snc2 protein and consistent with localization to prospore membrane precursor vesicles (unpublished data).

An alternative possibility is the existence of a sporulation-specific protein whose interaction with Sso1 and/or Snc2 is sensitive to these mutations. As Sec9 works with these proteins in vegetative cells and Spo20 replaces it during sporulation, Spo20 would be a candidate for such a factor. To test the possibility that the switch to Spo20 during sporulation is the basis for the *sso1*^{Q224X} phenotypes, we examined the ability of chimeras in

which the helices of Spo20 are replaced with those of Sec9 (*PSPS*) to rescue the *sso1*^{Q224R} sporulation defect. Strain HI3 (*sso1Δ/sso1Δ spo20Δ/spo20Δ*) carrying *pssso1*^{Q224R} was transformed with an empty vector, or one carrying *snc2*^{R52Q}, as well as high copy plasmids expressing either wild-type *SPO20* or the *PSPS* chimera. Expression of *snc2*^{R52Q} or *SPO20* alone did not increase the frequency of sporulation and, similarly, co-overexpression of *snc2*^{R52Q} and *SPO20* had no effect. Expression of *PSPS* alone resulted in some increase of sporulation; however, coexpression of both *snc2*^{R52Q} and the *PSPS* chimera resulted in sporulation at levels comparable to the same strain carrying *SSO1* and *SPO20* plasmids (Fig. 4). This result demonstrates that *snc2*^{R52Q} can contribute to suppression of *sso1*^{Q224R}, indicating that Snc2 does participate in fusion at the prospore membrane. Moreover, in the context of the rearranged central layer, the partner SNARE for Sso1/Snc2 must contain the Sec9 helical domains for sporulation to occur. Spo20 cannot support membrane assembly under these circumstances. Sensitivity of Spo20-containing complexes to perturbations of the ionic layer may also explain the sporulation-specific nature of other *sso1*^{Q224X} mutations.

To more precisely define the differences between Sec9 and Spo20 in their ability to mediate fusion in the context of *sso1*^{Q224R}/*snc2*^{R52Q}, the ability of chimeras replacing only one of the two Spo20 helices with that of Sec9 was examined. A swap of the first Spo20 helix (*PSPP*) was as effective at rescuing sporulation as the *PSPS* chimera. A swap of only the second helix (*PPPS*) also increased sporulation, but to a lesser extent than the first helix (Fig. 4). These results suggest that differences in the first helical domains of Spo20 and Sec9 are largely responsible for their differing phenotypes in this assay.

Mutation of two interface residues allows Spo20 to function with the altered Sso1/Snc2

In vitro, Sso1/Spo20–Snc2 complexes have a lower melting temperature than Sso1/Sec9–Snc2 complexes, suggesting that

<u>Ionic Layer</u>	<u>Configuration</u>	<u>Genes Expressed</u>	<u>% asci</u>	<u>Ether Test</u>
a		<i>SSO1 SPO20</i>	21.4	
b		<i>sso1^{Q224R} SPO20</i>	0.1	
a		<i>SSO1 PSPS</i>	20	
b		<i>sso1^{Q224R} PSPS</i>	4.65	
c		<i>sso1^{Q224R} snc2^{R52Q} SPO20</i>	0.55	
		<i>SSO1 snc2^{R52Q} PSPS</i>	17.6	
c		<i>sso1^{Q224R} snc2^{R52Q} PSPS</i>	11.8	
c		<i>sso1^{Q224R} snc2^{R52Q} PPPS</i>	6.2	
c		<i>sso1^{Q224R} snc2^{R52Q} PSPP</i>	14.3	
a				
b				
c				

Figure 4. Co-expression of *snc2^{R52Q}* and a chimeric *SPO20* rescues the sporulation defect of *sso1^{Q224R}*. Strain HJ3 (*sso1Δ/sso1Δ spo20Δ/spo20Δ*) was transformed with plasmids carrying the indicated genes and sporulated in liquid culture. *SSO1* alleles were expressed from CEN plasmids; *SNC2* and *SPO20* alleles were expressed from high copy plasmids. Sporulation was assessed by observation in the light microscope or by ether test. To determine percentage of sporulation, at least 500 cells were counted for each strain; percentages represent the average of four experiments. "a", "b", and "c" illustrate the arrangement of side chain residues at the ionic layer in the different strains.

Spo20 binds less tightly to these other SNAREs than does Sec9 (Liu et al., 2007). Packing interactions between side chains of amino acids located at interfaces on the SNARE helices are likely to determine how tightly the SNAREs in a given complex bind to each other. We aligned the interface residues of Spo20 and Sec9 to look for possible suboptimal residues in Spo20 (Fig. 5). As criteria to identify such residues, we looked for differences in the size and/or chemical properties of the side chains. In the first helix, only two positions looked significantly different, a cysteine at the +3 layer of Spo20 that is leucine in Sec9, and a serine at +5 that is an asparagine in Sec9. In the second helix, four differences of note were found; phenylalanines at the -2 and -1 layers that are threonine and leucine, respectively, in Sec9, an alanine in the +4 layer (leucine in Sec9) and a lysine residue at the +6 position (asparagine in Sec9). These six residues were mutated in pairs in the context of an otherwise wild-type *SPO20* sequence. The resulting mutants, *SPO20^{C224L,S231N}*, *SPO20^{F357L,F361T}*, and *SPO20^{A378L,K385N}* were all capable of rescuing the sporulation defect of a *spo20* mutant, indicating that the mutants encode functional proteins (unpublished data). They were then tested for their ability to rescue the sporulation defects of HJ3 (*sso1Δ/sso1Δ spo20Δ/spo20Δ*) expressing the *sso1^{Q224R}* and *snc2^{R52Q}* alleles (Fig. 5).

When sporulation was assessed on solid medium, the differences between the *PSPP* and *PPPS* chimeras were more pronounced than in liquid sporulation (Fig. 4). Consistent with

the relative ability of the different chimeras to promote sporulation, the alterations in the second helix, *SPO20^{F357L,F361T}* and *SPO20^{A378L,K385N}* had little effect on suppression, though *SPO20^{F357L,F361T}* did display a reproducible, slight improvement in sporulation efficiency. In contrast, *SPO20^{C224L,S231N}* allowed sporulation at a level comparable to the *PSPP* chimera, indicating that these two residues are primarily responsible for the ability of this chimera to function in conjunction with *sso1^{Q224R}* and *snc2^{R52Q}*.

SPO20^{C224L,S231N} can rescue *sec9-4^{ts}*

Ectopic expression of *SPO20* cannot rescue the temperature-sensitive growth defect of a *sec9-4* mutant, though a chimeric form of Spo20 carrying the Sec9 helical regions can rescue *sec9-4* (Neiman et al., 2000). This suggests that the inability of Spo20 to function at the plasma membrane is tied directly to its SNARE domain. We examined whether the *SPO20^{C224L,S231N}* allele affects the ability of Spo20 to compensate for loss of *SEC9*. These experiments were performed with proteins lacking the inhibitory domain (amino acids 3–51) present in the N terminus of Spo20 (Neiman et al., 2000). As previously reported, Δ 3-51*SPO20* cannot rescue *sec9-4*, even when present on a high copy plasmid, though Δ 3-51*PSPPS* was capable of rescuing growth at high temperature. The Δ 3-51*SPO20^{C224L,S231N}* allele also rescued growth of this strain at 37°C when present in high copy, though neither *SPO20^{C224L,S231N}* nor the *PSPP* chimera could rescue when

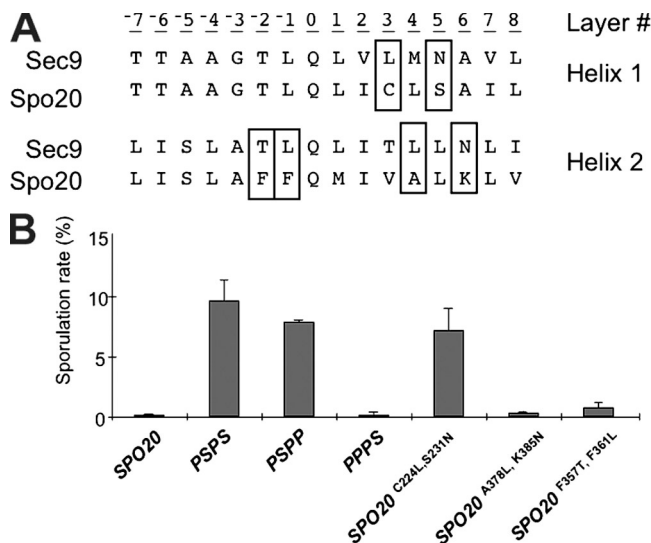


Figure 5. **Mutation of two interface residues in the Spo20 SNARE helix allows it to function with *sso1*^{Q224R}.** (A) Alignment of the interface residues in the SNARE domains of Spo20 and Sec9. Residues chosen for mutation are in blocks. (B) Sporulation of *sso1*^{Q224R} *snc2*^{R52Q} strains expressing different forms of *SPO20*. Strain HJ3 (*sso1* Δ /*sso1* Δ *spo20* Δ /*spo20* Δ) was transformed with plasmids carrying *sso1*^{Q224R} and *snc2*^{R52Q} as well as the indicated form of *SPO20*. The *sso1*^{Q224R} allele was expressed from a CEN plasmid; *snc2*^{R52Q} and the *SPO20* alleles were expressed from high copy plasmids. These strains were sporulated and sporulation efficiency measured in the light microscope. At least 500 cells were scored for each strain. Results are the average of three experiments. Error bars indicate one standard deviation.

expressed from centromeric plasmids (Fig. 6). These results again suggest that the *SPO20*^{C224L,S231N} mutations increase the strength of Spo20/Sso/Snc interactions, though not to the same degree as complete replacement with the Sec9 helices. To ensure the differences seen were not due to differential stability of the proteins, 3xHA-tagged versions of the different *SPO20* and chimera genes were constructed. Western blotting with anti-HA antibodies indicated that all the *SPO20* forms were present in comparable amounts (unpublished data). Therefore, the results reflect differences in the ability of the different forms to promote vesicle fusion, not differences in protein stability.

Mutation of *SPO20* increases association with Sso1 and Snc2 in vivo

If alteration of the SNARE helices of Spo20 increases its affinity for its partner SNAREs, this should be reflected in increased binding of the protein to Sso1 and Snc2. To address this possibility, HA-tagged Δ 50-Spo20, Spo20^{C224L,S231N}, or PSPS were expressed in combination with either wild-type Sso1 and Snc2 or Sso1^{Q224R} and Snc2^{R52Q} in a *sso1 sso2* strain. Lysates were made from each strain and the Spo20 proteins immunoprecipitated using anti-HA antibodies. Immunoprecipitates were then blotted and probed with anti-HA, anti-Sso1, or anti-Snc2 antibodies to examine association of the three SNARE proteins (Fig. 7). In the presence of both the wild-type and mutant Sso1 and Snc2 proteins the same pattern was seen; the PSPS chimera precipitated significantly more Sso1 and Snc2 than Spo20^{C224L,S231N}, which in turn brought down slightly more Sso1 and Snc2 than the wild-type Spo20. Though these immunoprecipitations do not provide

a direct measure of affinity, the increased association of PSPS and Spo20^{C224L,S231N} with both forms of Sso1 and Snc2 are consistent with the idea that they bind more avidly to their partner SNAREs than wild-type Spo20. Interestingly, all three forms of Spo20 exhibited greater association with the Sso1^{Q224R} and Snc2^{R52Q} proteins than with the wild-type SNAREs. Because the amount of SNAREs in complex reflects both the rates of assembly and of disassembly, we suggest that the general increase in the amount of SNARE complexes seen with Sso1^{Q224R}/Snc2^{R52Q} might reflect a role for the central ionic layer in complex disassembly, as suggested previously (Scales et al., 2001).

SPO20^{C224L,S231N} improves function of the SNARE complex in vitro

Studies of Sec9- and Spo20-containing SNARE complexes in an in vitro liposome fusion system indicate that, in a given lipid composition, Spo20-containing complexes are less fusogenic than Sec9 complexes (Liu et al., 2007). Moreover, this lesser activity correlates with decreased SNARE complex stability (measured as a lower melting temperature) of the Spo20 complexes compared with Sec9 complexes. The behavior of the *SPO20*^{C224L,S231N} mutant in the genetic tests and immunoprecipitations described above suggests that these mutations might increase the binding energy of the Spo20-containing complexes. To test this directly, the recombinant SNARE domain (amino acids 147–397) of Spo20^{C224L,S231N} was purified from *Escherichia coli* and tested with the Sso1 and Snc2 proteins in a liposome fusion assay. Using liposomes containing 85% POPC (palmitoyl oleoyl phosphatidylcholine) and 15% DOPS (di-oleoyl phosphatidylserine), Sso1/Sec9–Snc2 complexes promote liposome fusion at a greater rate than the Sso1/Spo20–Snc2 SNAREs (Fig. 8 A). In contrast, Sso1/Spo20^{C224L,S231N}–Snc2 mediates fusion at a rate comparable to the Sec9 complexes. Thus, parallel to the in vivo results, Spo20^{C224L,S231N} promotes fusion more efficiently than Spo20 in vitro.

To determine if the increased fusion activity was reflected in increased binding energy, the stability of the Spo20^{C224L,S231N}-containing complexes was examined. We previously reported that Sec9-containing complexes are significantly more stable than Spo20 complexes during equilibrium unfolding reactions with chemical denaturants where the concentration of Guanidinium-HCL required to disrupt 50% of the ternary SNARE complex was reduced 2.1M for Sec9 vs. 0.9M for Spo20 (Liu et al., 2007). When the Spo20^{C224L,S231N}-containing SNAREs were examined, a concentration of 1.1M Guanidinium-HCL disrupted 50% of these ternary complexes, indicating that they were more stable than those with Spo20, though still well below the stability of Sec9 complexes (Fig. 8 B). This moderate improvement in stability of the Spo20^{C224L,S231N}-containing complexes is consistent with the slight increase in binding of Spo20^{C224L,S231N} to Sso1 and Snc2 seen in the IP experiments (Fig. 7). Together with the liposome fusion data, these results suggest that modest changes in affinity can have strong effects on the fusogenic properties of the SNAREs. For the neuronal SNARE SNAP-25 it has similarly been found that mutation of interface residues can result in large differences in function while only modestly altering stability of the SNARE complex (Sorensen et al., 2006).

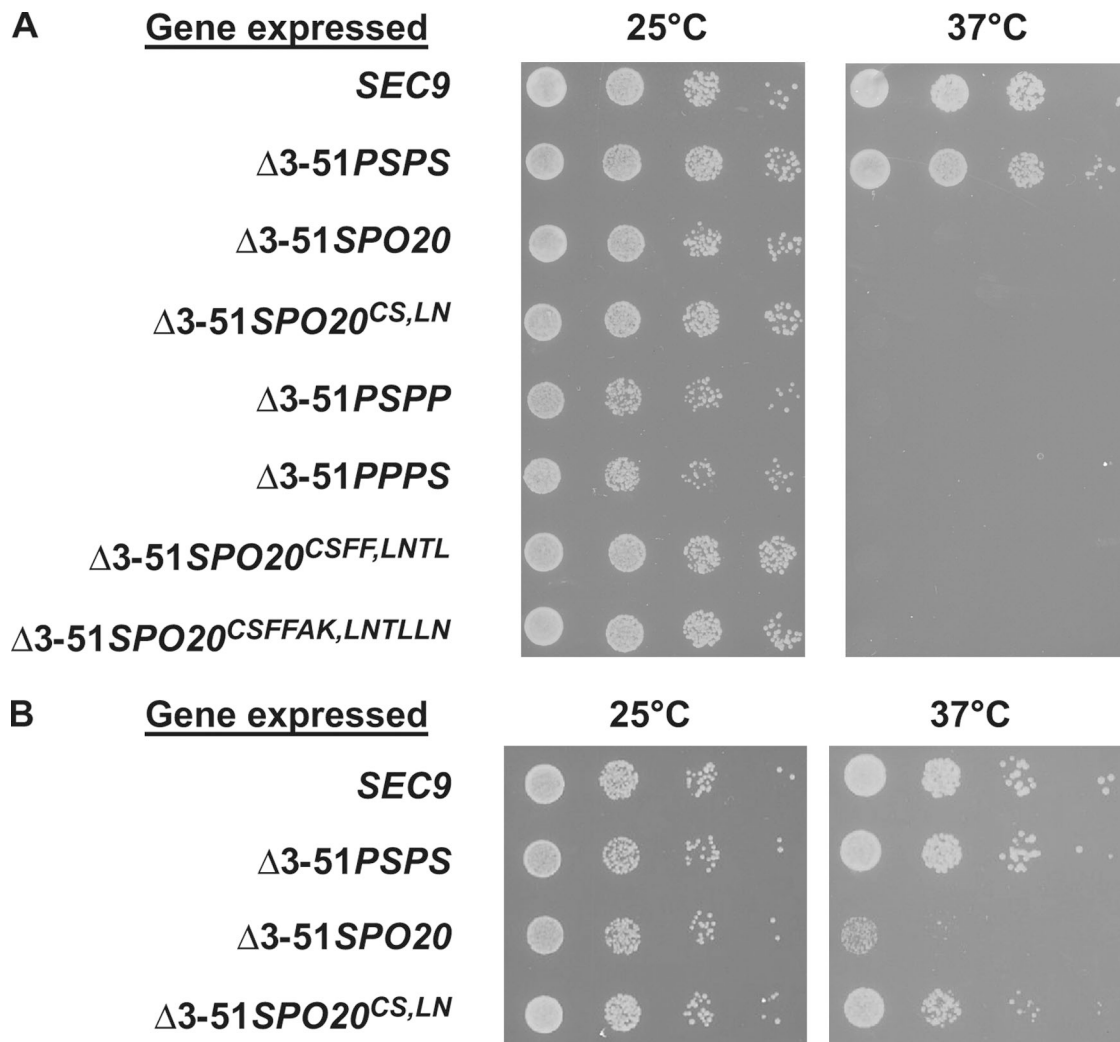


Figure 6. **SPO20^{C224L, S231N} can rescue the growth defect of sec9-4.** (A) Strain AN211 (*sec9-4*) was transformed with integrating or centromeric (for *PSPP* and *PPPS*) plasmids expressing the indicated genes. Cells were grown to saturation in rich medium and 10-fold serial dilutions were spotted onto selective plates incubated at permissive (25°C) or restrictive (37°C) temperature. *SPO20^{CS, LN}* is *SPO20^{C224L, S231N}*; *SPO20^{CSFF, LNTL}* is *SPO20^{C224L, S231N, F357T, F361L}*; *SPO20^{CSFFAK, LNTLLN}* is *SPO20^{C224L, S231N, F357T, F361L, A378K, K385N}*. (B) A similar growth assay in strain AN211 (*sec9-4*) using high copy plasmids to express the indicated genes.

Discussion

The use of compensatory mutations in the central ionic layer of the SNARE domain has proven to be an effective means to demonstrate the participation of different SNARE proteins in the same complex in vivo (Graf et al., 2005). Here, we attempted to use this technique to demonstrate a role for the Snc1/2 proteins in fusion at the prospore membrane. A compensatory mutation in *SNC2* could only rescue the sporulation defect of *sso1^{Q224R}* when expressed in concert with forms of Spo20 carrying the Sec9 SNARE helices. Similar results were obtained using a compensatory mutation in *SNC1* (unpublished data). These results demonstrate, first, that the Snc1 and Snc2 proteins indeed function as the R-SNARE subunit of the prospore membrane SNARE complex and, second, that placement of the central layer arginine in different helices is not functionally equivalent. In this instance, swapping the glutamine and arginine between the Sso1 and Snc2 helices creates a SNARE bundle that is more sensitive to the composition of other interface layers in the complex. When

Spo20 is the partner, the binding energies at other interfaces are insufficient to overcome the weaker central layer interactions.

During the course of this work, a crystal structure of the SNARE complex containing the Sso1, Snc2, and Sec9 helical domains was published (Strop et al., 2008). When this structure is used to model in the Spo20 cysteine and serine side chains at the +3 and +5 interface layers, the Spo20 residues result in an apparent loss of packing interactions between the side chains (unpublished data), consistent with our results indicating that the Sec9 residues at these positions improve stability of the SNARE complex. Mutational analysis of interface residues in SNAP-25 revealed that interactions in the N-terminal half of the SNARE domain are important for promoting priming or docking of the vesicle, whereas interactions in the C-terminal half of the SNARE helix are critical to drive membrane fusion (Sorensen et al., 2006). In this regard, it is noteworthy that the critical interfaces differentiating the ability of Spo20 and Sec9 to promote fusion at the plasma membrane lie in the C-terminal domain, suggesting that fusion and not docking is the affected step.

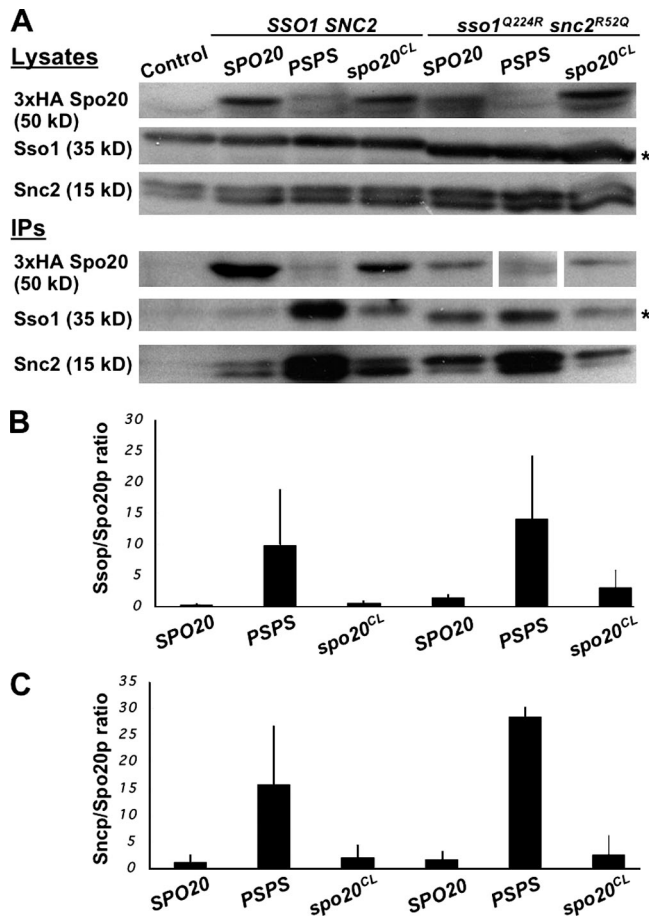


Figure 7. Mutation of the Spo20 helices increases binding of Sso1 and Snc2. Strain HI75 (*ssolΔ sso2Δ*) was transformed with high copy plasmids expressing 3xHA tagged forms of Δ3-51Spo20, Δ3-51Spo20^{C224L S231N}, or Δ3-51PSPS chimera. Additionally, these cells carried a CEN plasmid expressing either *SSO1* or *SSO1*^{Q224R} and high copy plasmids expressing *SNC2* or *SNC2*^{R52Q}, respectively. These strains were grown to mid-log in selective medium, lysed, and the HA-tagged Spo20 proteins immunoprecipitated. (A) (top) Western blots of cell lysates from each strain probed with anti-HA, anti-Sso1, or anti-Snc2 antibodies. 3X-HA indicates bands corresponding to the different Spo20 mutants; (bottom) Western blots of anti-HA immunoprecipitates from the same lysates. The band corresponding to Δ3-51PSPS in the *Sso1*^{Q224R}/*Snc2*^{R52Q} strain is shown from a longer exposure of the same blot. Asterisk indicates *Sso1*^{Q224R}, which displays slightly increased mobility compared with the wild-type *Sso1*. (B) Quantitation of the coprecipitation of Sso1 proteins with the different forms of Spo20. Amounts are expressed as the ratio of Sso1 to Spo20 protein based on relative intensity of bands on the anti-HA and anti-Sso1 blots. Values shown are the average of three experiments. Bars indicate one standard deviation. (C) Quantitation of the coprecipitation of Snc2 proteins with the different forms of Spo20. Amounts are expressed as the ratio of Snc2 to Spo20 protein based on relative intensity of bands on the anti-HA and anti-Snc2 blots. Values shown are the average of three experiments. Bars indicate one standard deviation.

Again, this is consistent with the results we observe in the liposome fusion assay.

Role of the central ionic layer

Our results raise questions about the function of the central ionic layer present in all SNARE complexes. We found that vegetative secretion was remarkably insensitive to mutation of the glutamine found at this layer in Sso1. Mutation to proline, which would likely disrupt the SNARE helix, or to arginine or lysine, which

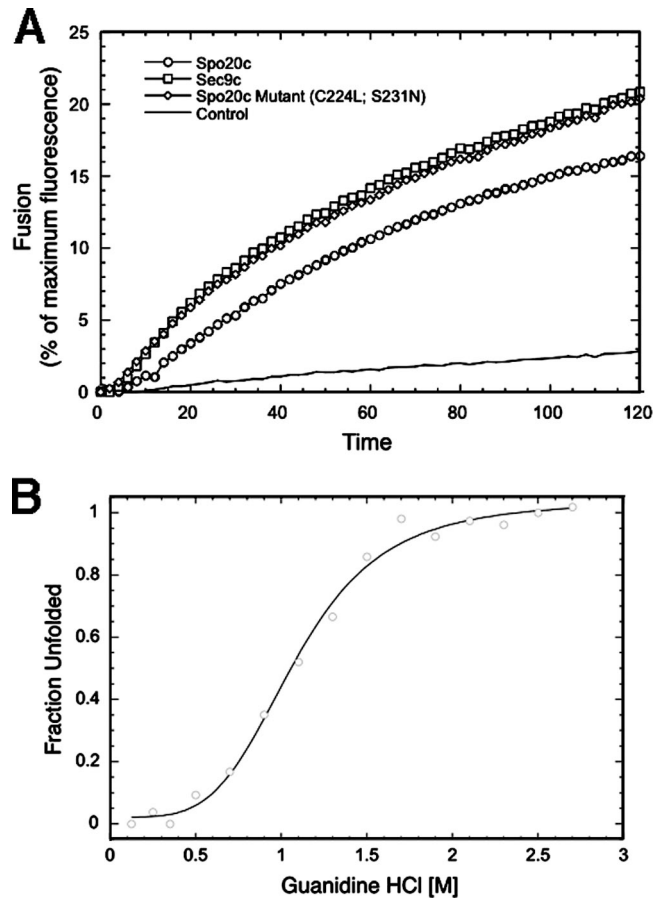


Figure 8. Spo20^{C224L,S231N} is a more efficient fusogen in vitro. (A) Liposome fusion assay. Liposomes containing Sso1 and the SNARE domains of Sec9, Spo20, or Spo20^{C224L,S231N} were mixed with Snc2-containing liposomes and fusion assayed by fluorescence. (B) Stability of Sso1/Snc2/ Spo20^{C224L,S231N} complexes in increasing concentrations of Guanidinium-HCl.

would introduce positive charges that clash with the arginine on the Snc2 helix, reduced or eliminated function. However, any other amino acid at this position was well tolerated. This is quite surprising in light of the strong conservation of this glutamine in all syntaxin-family SNARE proteins (Bock et al., 2001). Our results with Spo20 suggest one possible explanation for this apparent paradox. The sensitivity of Spo20-containing complexes to alteration of glutamine 224 would provide selective pressure for its maintenance in Sso1. It may be that other SNARE complexes more closely resemble Spo20- than Sec9-containing SNAREs and are sensitive to perturbation of the central ionic layer.

The ability of mutant forms of Sso1 to function well raises the question of the conservation not just of the glutamine residue, but also of the ionic layer. The ionic layer has been shown to be important for efficient disassembly of the neuronal SNARE complex in vitro (Scales et al., 2001), and our immunoprecipitation data are consistent with this idea. However, the lack of growth phenotype of the *SSO1*^{Q224} mutations suggests that disassembly must still occur with reasonable efficiency in the mutants. Another suggested explanation is that the ionic layer allows the multiple helices to assemble in the appropriate register (Fasshauer et al., 1998). Examination of the interface residues in defined SNARE complexes reveals that interfaces with one or two polar

Table 1. Strains used in this study

Strain	Genotype	Source
HI3	<i>MATa/MATa ura3/ura3 trp1/trp1 leu2/leu2 his3/his3 lys2/lys2 arg4/ARG4 rme1ΔLEU2/RME1 hoΔLYS2/hoΔLYS2 sso1Δhis5⁺/sso1Δhis5⁺</i>	This study
HI75	<i>MATa/MATa ura3/ura3 trp1/trp1 leu2/leu2 his3/his3 met15/MET15 arg4/ARG4 sso1Δhis5⁺/sso1Δhis5⁺ sso2Δkan^r/sso2Δkan^r pRS316-SSO1</i>	This study
HJ3	<i>MATa/MATa ura3/ura3 trp1/trp1 leu2/leu2 his3/his3 sso1Δkan^r/sso1Δkan^r spo20Δhis5⁺/spo20Δhis5⁺</i>	This study
AN211	<i>MATa/MATa ura3/ura3 trp1/trp1 leu2/leu2 his3/his3 lys2/LYS2 ade2/ADE2 s9-4/sec9-4 spo20Δhis5⁺/spo20Δhis5</i>	Nakanishi et al., 2004

residues are not uncommon. However a charged residue or more than two polar residues is quite rare (unpublished data). In our experiments, three of the four helices still contain polar or charged residues (two glutamines and an arginine). Therefore, this may still provide sufficient information to assemble the complex in register. Though mutation of all the central ionic layers to hydrophobic residues did not disrupt assembly of the neuronal SNARE complex in vitro (Scales et al., 2001), it would be interesting to determine if combining additional ionic layer changes with *SSO1*^{Q224} changes in the yeast SNARE would result in a much more severe fusion defect.

Control of SNARE specificity in vivo

The switch from Sec9- to Spo20-dependent fusion during sporulation provides an excellent system to explore the mechanisms by which a change in a single SNARE subunit can alter the target specificity of a particular class of vesicle. Our results here, along with those previously reported, allow us to answer this question. The specificity of Sec9 and Spo20 for their respective membranes is reinforced in three ways. First, transcriptional control, in wild-type cells *SPO20* is transcribed only during sporulation and so cannot function in constitutive secretion (Neiman, 1998). The second mechanism is control of intracellular localization. Efficient targeting of Sec9 to the prospore membrane, either by fusing it to the Spo20 lipid binding motif or to an integral membrane protein, allows Sec9 to restore some degree of sporulation to *spo20* cells (Neiman et al., 2000; Nakanishi et al., 2006). Finally, as we show here, SNARE specificity can be controlled by the strength of the binding interactions between the SNAREs themselves. As the binding energy required for a given fusion event will depend on the potential energy barrier to fusion of the two membranes involved, this form of regulation is linked to the lipid composition of the membranes.

Control of localization and strength of binding are likely to be general mechanisms contributing to SNARE specificity. In liposome binding experiments, the R-SNARE Sec22 is capable of mediating fusion in concert with Sso1 and Sec9 (McNew et al., 2000). This result has been suggested to indicate the existence of a direct ER-to-plasma membrane secretion step in yeast, as found in mammalian cells (Becker et al., 2005). Alternatively, it may be that, though Sec22 is capable of forming productive complexes with Sso1 and Sec9, it does not do so because its localization as a v-SNARE is limited to the cis Golgi- and ER-directed vesicles that do not dock with the plasma membrane in vivo. Consistent with this idea, overexpression of a Sec22^{R157Q} mutant cannot

rescue sporulation of the Sso1^{Q224R} mutant even in the presence of the PSPS chimera (unpublished data), suggesting that Sec22 cannot participate in prospore membrane fusion events in vivo.

A recent study revealed that a suboptimal interface at the +7 layer in the neuronal *syx-1A* gene is important for allowing calcium-mediated regulation of secretion (Lagow et al., 2007). Mutation of the threonine residue at this position in *syx-1A* to the corresponding isoleucine residue in *syx-2* led to constitutive fusion. Thus, as with Spo20 and Sec9, in the neuronal SNARE complex tuning of the strength of binding interactions is important for allowing proper regulation of vesicle transport.

Finally, Spo20 and Sec9 provide a useful model for the evolution of novel SNARE complexes. During the evolution of *Saccharomyces*, a whole genome duplication occurred that ultimately gave rise to many related gene pairs in the *S. cerevisiae* genome (Wolfe and Shields, 1997). Sec9 and Spo20 arose from this duplication event. In yeasts that diverged from the *S. cerevisiae* lineage before the duplication, such as *Schizosaccharomyces pombe*, a single Sec9/Spo20 related gene participates in fusion at both the plasma membrane and the prospore membrane (Nakamura et al., 2005). Thus, in the *S. cerevisiae* lineage, the duplication event allowed the two paralogues to become specialized for action at distinct compartments where the ancestral protein functioned at both membranes. Similar patterns are likely at work in the expansions of particular SNARE families seen in plant and mammalian genomes (Sanderfoot et al., 2000; Bock et al., 2001).

Materials and methods

Yeast strains and genetics methods

Unless otherwise noted, standard media and genetic methods were used (Rose and Fink, 1990). The strains used in this study are listed in Table 1. Strain HI3 was constructed by PCR-mediated replacement (Longtine et al., 1998) of the *SSO1* gene in the haploid strains AN117-4B and AN117-16D (Neiman et al., 2000) and mating of the resulting haploids. Strain HI75 was constructed by mating the *sso1Δhis5⁺* derivative of AN117-4B to an *sso2Δkan^r* strain from the *S. cerevisiae* knockout collection (Winzeler et al., 1999). The resulting diploid was transformed with pRS316-SSO1 and then sporulated. Segregants lacking both *SSO1* and *SSO2* were then mated to generate HI75. To construct strain HJ3, a strain from the *S. cerevisiae* knockout collection carrying the *sso1Δkan^r* allele was first mated to AN117-4B. A haploid segregant from this cross was mated to strain AN1052 (Neiman et al., 2000), and this diploid was dissected and double mutant *sso1Δ spo20Δ* haploids were mated.

Plasmids

Plasmids used in this study are listed in Table II. Plasmids pRS314-SSO1 and pRS314-*sso1*^{Q224R} were constructed by digesting pRS316-SSO1 and pRS316-*sso1*^{Q224R} (Katz and Brennwald, 2000) with PvuII. These fragments were cotransformed into yeast with KpnI-SacI-digested pRS314 (Sikorski and Hieter, 1989), and the reconstituted plasmids were recovered from yeast. To construct the other glutamine 224 substitutions, the *sso1*^{Q224R} gene

Table II. Plasmids used in this study

Name	Source
pRS314	Sikorski et al., 1989
pRS314-SSO1	This study
pRS314- <i>sso1</i> ^{Q224R}	This study
pRS425	Christianson et al., 1992
pRS425- <i>snc2</i> ^{R52Q}	This study
pRS426	Christianson et al., 1992
pRS426-SPO20	Nakanishi et al., 2004
pRS426-PSPS	This study
pRS426-PSPP	This study
pRS426-PPPS	This study
pRS426-SPO20 ^{C224L,S231N}	This study
pRS426-SPO20 ^{F357T,F361L}	This study
pRS426-SPO20 ^{A378L,K385N}	This study
pRS306-SEC9pr-SEC9	Neiman et al., 2000
pRS306-SEC9pr-Δ3-51 SPO20	This study
pRS306-SEC9pr-Δ3-51 PSPS	This study
pRS306-SEC9pr-Δ3-51 SPO20 ^{C224L,S231N}	This study
pRS306-SEC9pr-Δ3-51 SPO20 ^{C224L,S231N,F357T,F361L,A378L,K385N}	This study
pRS316-SEC9pr-Δ3-51 PSPP	This study
pRS316-SEC9pr-Δ3-51 PPPS	This study
pRS426-SEC9pr-SEC9	This study
pRS426-SEC9pr-Δ3-51 SPO20	This study
pRS426-SEC9pr-Δ3-51 PSPS	This study
pRS426-SEC9pr-Δ3-51 SPO20 ^{C224L,S231N}	This study
pRS426-SEC9pr-Δ3-51 PSPP	This study
pRS426-SEC9pr-Δ3-51 PPPS	This study
pRS426-SEC9pr-3xHA SEC9	This study
pRS426-SEC9pr-3xHA Δ3-51 SPO20	This study
pRS426-SEC9pr-3xHA Δ3-51 PSPS	This study
pRS426-SEC9pr-3xHA Δ3-51 SPO20 ^{C224L,S231N}	This study
pRS426-SEC9pr-3xHA Δ3-51 SPO20 ^{F357T,F361L}	This study
pRS426-SEC9pr-3xHA Δ3-51 PSPP	This study
pRS426-SEC9pr-3xHA Δ3-51 PPPS	This study

was first cloned as a BamHI–HindIII fragment from pRS314-*sso1*^{Q224R} into similarly digested pUC119. Site-directed mutagenesis was then performed using oligonucleotides ANO377 and ANO378, which contain randomized nucleotides at codon 224. Sequencing of individual clones from the mutagenesis identified particular substitutions. All substitutions except lysine, glutamine, histidine, and aspartate were obtained in this way. For lysine, glutamine, and histidine, the randomized oligos HNO961 and HNO962 were used. For aspartate, mutagenesis was performed using oligos HNO991 and HNO992. After specific mutations were identified by sequencing, the 3' end of the SSO1 gene carrying the glutamine 224 substitution was swapped into pRS314-SSO1 as an NcoI–SalI fragment. To construct the pRS426 and pRS316 plasmids expressing the chimeras PSPS, PSPP, and PPPS, SacI–KpnI fragments carrying the SPO20 promoter and the indicated chimera were isolated from the corresponding integrating plasmids (Neiman et al., 2000) and cloned into similarly digested pRS426 or pRS316, respectively (Sikorski and Hieter, 1989; Christianson et al., 1992). To construct pRS425-*snc2*^{R52Q} a BamHI–SalI fragment carrying the *snc2*^{R52Q} gene (Katz and Brennwald, 2000) was cloned into BamHI–SalI-digested pRS426.

To make pRS316-SEC9pr-PSPP and pRS316-SEC9pr-PPPS, SpeI–SacI fragments carrying the particular chimera were excised from pRS426-SPO20pr-PSPP or -PPPS and cloned into the backbone of SpeI–SacI-digested pRS316-SEC9pr-PSPS (Nakanishi et al., 2004). The plasmids pRS426-SPO20pr-SPO20^{C224L,S231N}, pRS426-SPO20pr-SPO20^{A378L,K385N}, and pRS426-SPO20pr-SPO20^{F357T,F361L} were created by site-directed mutagenesis of the plasmid pRS426-SPO20pr-SPO20 (Nakanishi et al., 2004) using oligos HJO31 and HJO32, HJO33 and HJO34, and HJO35 and HJO36, respectively.

Integrating plasmids expressing Δ3-51 SPO20 and Δ3-51 SPO20^{C224L,S231N} under the SEC9 promoter were assembled by amplifying

the genes from pRS426-SPO20pr-SPO20 and pRS426-SPO20pr-SPO20^{C224L,S231N}, respectively, using oligos BBO14 and ANO168. The PCR products were digested with XhoI and SacI, and cloned into similarly digested pRS306-SEC9pr (Neiman et al., 2000). To make the sextuple mutant SPO20^{C224L,S231N,F357T,F361L,A378L,K385N}, pRS306-SEC9pr-Δ3-51 SPO20^{C224L,S231N} was used as template for site-directed mutagenesis using first primers HJO33 and HJO34, and then HJO35 and HJO36. To construct 2 μ plasmids expressing the various SPO20 mutants and SPO20/SEC9 chimeras under SEC9 promoter control, KpnI–SacI fragments containing SEC9 promoter with indicated genes were cloned from the integrating and CEN plasmids into KpnI and SacI sites of pRS426.

To construct 3xHA tagged versions of the different SPO20 mutants, two complementary oligos (HJO72 and HJO73) were synthesized that encode 3 HA epitopes and anneal to leave XhoI-compatible ends. The oligos were phosphorylated with T4 polynucleotide kinase (Invitrogen) at 37°C for 10 min, mixed, and then allowed to anneal. The annealed oligos were then ligated with XhoI-digested pRS306-SEC9pr-SEC9 (Neiman et al., 2000). Site-directed mutagenesis was then performed using oligos HJO78 and HJO79 to restore an XhoI at the junction of 3xHA and SEC9. Finally, an XhoI–SacI fragment containing SEC9 was replaced with the corresponding XhoI–SacI fragments from pRS306-SEC9pr-Δ3-51 SPO20, Δ3-51 SPO20^{C224L,S231N}, or Δ3-51 SPO20/SEC9 chimera plasmids.

Sporulation assays

Sporulation assays were performed as described previously (Neiman et al., 2000). For tests on solid medium, the strains to be tested were grown overnight on selective media, and then replica plated to sporulation medium. After 24 h, spore formation was quantified by direct observation in the light microscope.

For liquid sporulation and ether tests, 1.5 ml of overnight-cultured cells were pelleted, washed once in 1 ml 2% potassium acetate, and resuspended in 10 ml 2% potassium acetate. After 2 d of incubation at 30°C, the sporulation frequency was determined by observation under the light microscope; meanwhile, 5 µl of the culture was spotted onto a YPD plate. The plate was inverted over a paper filter soaked with 2 ml of ethyl ether for 30 min. After 30 min the paper filter was removed, and the plate was incubated at 30°C overnight.

Growth assays

To assay the growth defect of the *spo20Δ sec9-4* mutant, cells were first cultured overnight at 25°C in YPD. Thereafter, 10-fold serial-diluted cell cultures were spotted onto two identical plates selective for the plasmid. One plate was placed at 25°C, and the other at 37°C to monitor the growth rate of the *spo20Δ sec9-4* mutant.

Immunoprecipitations

The immunoprecipitation assays were modified from Carr et al. (1999). Strain HI75 was transformed with *CEN* plasmids expressing the different *SSO1* genes and high copy plasmids expressing the different *SNC2* and *SPO20* alleles. 5 ml of overnight culture was diluted into 100 ml of selective medium and grown to mid-log phase. Cells were harvested and resuspended in 1 ml of ice-cold wash buffer (20 mM Tris, pH 7.5, 20 mM Na₃N, and 20 mM NaF). Washed cells were pelleted at 4°C, resuspended in 1 ml ice-cold IP buffer (50 mM Hepes, pH 7.4, 150 mM KCl, 1 mM EDTA, 1 mM DTT, and 0.5% NP-40), and treated with zymolyase (100 µg/ml) for 10 min. Cells were pelleted and resuspended in 500 µl ice-cold IP buffer with protease inhibitors. Cells were lysed by shaking with glass beads (0.5 mm) at 4°C for 10 min. Lysed cells were pelleted for 10 min at 13,000 g and the supernatants were precleared by addition of protein G–Sepharose beads (GE Healthcare). The mixtures were rocked for 30 min at 4°C and then centrifuged for 15 min at 13,000 g at 4°C to pellet the beads, debris, and non-specifically bound products. To precipitate the HA-tagged proteins, anti-HA monoclonal antibodies (clone HA-7; Sigma-Aldrich) were added to the pre-cleared supernatants for 30 min before G–Sepharose beads were added, and the mixtures were incubated at 4°C overnight. The beads and bound protein were pelleted for 10 s at 4,000 g, and washed five times with 1 ml ice-cold IP buffer. Proteins were eluted from the beads by boiling them in 2X SDS sample buffer (60 mM Tris-HCl, pH 6.8, 10% glycerol, 2% SDS, 0.05 mg/ml bromophenol blue, and 5% β-mercaptoethanol) for 5 min.

Proteins of interest were analyzed by Western blot. 3xHA-Δ3-51Spo20 species were separated by SDS-PAGE on 10% mini-gels, whereas Sso1 and Snc2 were resolved on 15% mini-gels. Proteins were transferred to PVDF membranes (Millipore). 3xHA-Δ3-51Spo20 species were visualized with chicken anti-HA antibodies (Aves Laboratories) to minimize the cross-reactivity from the mouse HA antibodies in the IP. Sso1 and Snc2 were detected by rabbit anti-Sso1 and rabbit anti-Snc2 (Sogaard et al., 1994), respectively. Peroxidase-conjugated secondary antibodies (anti-chicken or anti-rabbit) were used. The band intensities were determined using ImageJ and the ratios of Sso1 or Snc2 to the precipitated 3xHA-Δ3-51Spo20 protein were calculated to compare coprecipitation of Sso1 and Snc2 with the different 3xHA-Δ3-51Spo20 species.

Protein expression and purification

Sso1, Snc1, Sec9, and Spo20 were expressed and purified as previously described in detail (Liu et al., 2007). Spo20^{C224L,S231N} was expressed and purified from pET24a(+)-based plasmid pJM557 as done previously for Spo20. The Spo20^{C224L,S231N} (147–397) fragment for pJM557 was amplified from pRS306SEC9pr::Δ50spo20^{C224L,S231N} using primers #303 [CCGAATTCGACTATCCACAGTGG] and #304 [GCACGCGTCTCGAGTACCATCTTTCCCG].

Liposome fusion assays

Liposome reconstitution and fusion assay were performed as described previously (Liu et al., 2007).

Melting temperature determination

The stability of Spo20^{C224L,S231N} ternary SNARE complex was determined by chemical denaturation using guanidine HCl as the denaturant. Changes in CD signal were performed using a spectrometer (model 62DS; Aviv) as described previously (Liu et al., 2007). The [GdnHCl]_{1/2} of the Spo20^{C224L,S231N} ternary SNARE complex was determined by KaleidaGraph (Synergy Software) using nonlinear least squares analysis.

Image acquisition and processing

Images of yeast growth and Western blots were acquired on a scanner (model 2450; Epson) and figures were prepared using Microsoft PowerPoint and Adobe Photoshop 9.0.

The authors wish to thank Pat Brennwald and Reinhard Jahn for plasmids.

This work was supported by National Institutes of Health grants GM62184 (to A.M. Neiman) and GM071832 (to J.A. McNew).

Submitted: 24 September 2008

Accepted: 11 November 2008

References

- Aalto, M.K., H. Ronne, and S. Keranen. 1993. Yeast syntaxins Sso1p and Sso2p belong to a family of related membrane proteins that function in vesicular transport. *EMBO J.* 12:4095–4104.
- Becker, T., A. Volchuk, and J.E. Rothman. 2005. Differential use of endoplasmic reticulum membrane for phagocytosis in J774 macrophages. *Proc. Natl. Acad. Sci. USA.* 102:4022–4026.
- Bock, J.B., H.T. Matern, A.A. Peden, and R.H. Scheller. 2001. A genomic perspective on membrane compartment organization. *Nature.* 409:839–841.
- Brennwald, P., B. Kearns, K. Champion, S. Keranen, V. Bankaitis, and P. Novick. 1994. Sec9 is a SNAP-25-like component of a yeast SNARE complex that may be the effector of Sec4 function in exocytosis. *Cell.* 79:245–258.
- Carr, C.M., E. Grote, M. Munson, F.M. Hughson, and P.J. Novick. 1999. Sec1p binds to SNARE complexes and concentrates at sites of secretion. *J. Cell Biol.* 146:333–344.
- Christianson, T.W., R.S. Sikorski, M. Dante, J.H. Shero, and P. Hieter. 1992. Multifunctional yeast high-copy-number shuttle vectors. *Gene.* 110:119–122.
- Coluccio, A., M. Malzone, and A.M. Neiman. 2004. Genetic evidence of a role for membrane lipid composition in the regulation of soluble NEM-sensitive factor receptor function in *Saccharomyces cerevisiae*. *Genetics.* 166:89–97.
- Fasshauer, D., R.B. Sutton, A.T. Brunger, and R. Jahn. 1998. Conserved structural features of the synaptic fusion complex: SNARE proteins reclassified as Q- and R-SNAREs. *Proc. Natl. Acad. Sci. USA.* 95:15781–15786.
- Graf, C.T., D. Riedel, H.D. Schmitt, and R. Jahn. 2005. Identification of functionally interacting SNAREs by using complementary substitutions in the conserved ‘0’ layer. *Mol. Biol. Cell.* 16:2263–2274.
- Jahn, R., and R.H. Scheller. 2006. SNAREs—engines for membrane fusion. *Nat. Rev. Mol. Cell Biol.* 7:631–643.
- Jantti, J., M.K. Aalto, M. Oyen, L. Sundqvist, S. Keranen, and H. Ronne. 2002. Characterization of temperature-sensitive mutations in the yeast syntaxin 1 homologues Sso1p and Sso2p, and evidence of a distinct function for Sso1p in sporulation. *J. Cell Sci.* 115:409–420.
- Katz, L., and P. Brennwald. 2000. Testing the 3Q:1R “rule”: mutational analysis of the ionic “zero” layer in the yeast exocytic SNARE complex reveals no requirement for arginine. *Mol. Biol. Cell.* 11:3849–3858.
- Lagow, R.D., H. Bao, E.N. Cohen, R.W. Daniels, A. Zuzek, W.H. Williams, G.T. Macleod, R.B. Sutton, and B. Zhang. 2007. Modification of a hydrophobic layer by a point mutation in syntaxin 1A regulates the rate of synaptic vesicle fusion. *PLoS Biol.* 5:e72.
- Liu, S., K.A. Wilson, T. Rice-Stitt, A.M. Neiman, and J.A. McNew. 2007. In vitro fusion catalyzed by the sporulation-specific t-SNARE light-chain Spo20p is stimulated by phosphatidic acid. *Traffic.* 8:1630–1643.
- Longtine, M.S., A. McKenzie III, D.J. Demarini, N.G. Shah, A. Wach, A. Brachat, P. Philippsen, and J.R. Pringle. 1998. Additional modules for versatile and economical PCR-based gene deletion and modification in *Saccharomyces cerevisiae*. *Yeast.* 14:953–961.
- McNew, J.A. 2008. Regulation of SNARE-mediated membrane fusion during exocytosis. *Chem. Rev.* 108:1669–1686.
- McNew, J.A., F. Parlati, R. Fukuda, R.J. Johnston, K. Paz, F. Paumet, T.H. Sollner, and J.E. Rothman. 2000. Compartmental specificity of cellular membrane fusion encoded in SNARE proteins. *Nature.* 407:153–159.
- Nakamura, T., J. Kashiwazaki, and C. Shimoda. 2005. A fission yeast SNAP-25 homologue, SpSec9, is essential for cytokinesis and sporulation. *Cell Struct. Funct.* 30:15–24.
- Nakanishi, H., P. de los Santos, and A.M. Neiman. 2004. Positive and negative regulation of a SNARE protein by control of intracellular localization. *Mol. Biol. Cell.* 15:1802–1815.
- Nakanishi, H., M. Morishita, C.L. Schwartz, A. Coluccio, J. Engebrecht, and A.M. Neiman. 2006. Phospholipase D and the SNARE Sso1p are necessary for vesicle fusion during sporulation in yeast. *J. Cell Sci.* 119:1406–1415.
- Neiman, A.M. 1998. Prospore membrane formation defines a developmentally regulated branch of the secretory pathway in yeast. *J. Cell Biol.* 140:29–37.
- Neiman, A.M. 2005. Ascospore formation in the yeast *Saccharomyces cerevisiae*. *Microbiol. Mol. Biol. Rev.* 69:565–584.

- Neiman, A.M., L. Katz, and P.J. Brennwald. 2000. Identification of domains required for developmentally regulated SNARE function in *Saccharomyces cerevisiae*. *Genetics*. 155:1643–1655.
- Oyler, G.A., G.A. Higgins, R.A. Hart, E. Battenberg, M. Billingsley, F.E. Bloom, and M.C. Wilson. 1989. The identification of a novel synaptosomal-associated protein, SNAP-25, differentially expressed by neuronal subpopulations. *J. Cell Biol.* 109:3039–3052.
- Parlati, F., J.A. McNew, R. Fukuda, R. Miller, T.H. Sollner, and J.E. Rothman. 2000. Topological restriction of SNARE-dependent membrane fusion. *Nature*. 407:194–198.
- Parlati, F., O. Varlamov, K. Paz, J.A. McNew, D. Hurtado, T.H. Sollner, and J.E. Rothman. 2002. Distinct SNARE complexes mediating membrane fusion in Golgi transport based on combinatorial specificity. *Proc. Natl. Acad. Sci. USA*. 99:5424–5429.
- Paumet, F., B. Brugger, F. Parlati, J.A. McNew, T.H. Sollner, and J.E. Rothman. 2001. A t-SNARE of the endocytic pathway must be activated for fusion. *J. Cell Biol.* 155:961–968.
- Paumet, F., V. Rahimian, and J.E. Rothman. 2004. The specificity of SNARE-dependent fusion is encoded in the SNARE motif. *Proc. Natl. Acad. Sci. USA*. 101:3376–3380.
- Pelham, H.R. 1999. SNAREs and the secretory pathway—lessons from yeast. *Exp. Cell Res.* 247:1–8.
- Poirier, M.A., W. Xiao, J.C. Macosko, C. Chan, Y.K. Shin, and M.K. Bennett. 1998. The synaptic SNARE complex is a parallel four-stranded helical bundle. *Nat. Struct. Biol.* 5:765–769.
- Protopopov, V., B. Govindan, P. Novick, and J.E. Gerst. 1993. Homologs of the synaptobrevin/VAMP family of synaptic vesicle proteins function on the late secretory pathway in *S. cerevisiae*. *Cell*. 74:855–861.
- Rose, M.D., and G.R. Fink. 1990. *Methods in Yeast Genetics*. Cold Spring Harbor Laboratory Press, Cold Spring Harbor, NY.
- Sanderfoot, A.A., F.F. Assaad, and N.V. Raikhel. 2000. The *Arabidopsis* genome. An abundance of soluble N-ethylmaleimide-sensitive factor adaptor protein receptors. *Plant Physiol.* 124:1558–1569.
- Scales, S.J., B.Y. Yoo, and R.H. Scheller. 2001. The ionic layer is required for efficient dissociation of the SNARE complex by a-SNAP and NSF. *Proc. Natl. Acad. Sci. USA*. 98:14262–14267.
- Sikorski, R.S., and P. Hieter. 1989. A system of shuttle vectors and yeast host strains designed for efficient manipulation of DNA in *Saccharomyces cerevisiae*. *Genetics*. 122:19–27.
- Sogaard, M., K. Tani, R.R. Ye, S. Geromanos, P. Tempst, T. Kirchhausen, J.E. Rothman, and T. Sollner. 1994. A rab protein is required for the assembly of SNARE complexes in the docking of transport vesicles. *Cell*. 78:937–948.
- Sollner, T., S.W. Whiteheart, M. Brunner, H. Erdjument-Bromage, S. Geromanos, P. Tempst, and J.E. Rothman. 1993. SNAP receptors implicated in vesicle targeting and fusion. *Nature*. 362:318–324.
- Sorensen, J.B., K. Wiederhold, E.M. Muller, I. Milosevic, G. Nagy, B.L. de Groot, H. Grubmuller, and D. Fasshauer. 2006. Sequential N- to C-terminal SNARE complex assembly drives priming and fusion of secretory vesicles. *EMBO J.* 25:955–966.
- Strop, P., S.E. Kaiser, M. Vrljic, and A.T. Brunger. 2008. The structure of the yeast plasma membrane SNARE complex reveals destabilizing water-filled cavities. *J. Biol. Chem.* 283:1113–1119.
- Sutton, R.B., D. Fasshauer, R. Jahn, and A.T. Brunger. 1998. Crystal structure of a SNARE complex involved in synaptic exocytosis at 2.4 Å resolution. *Nature*. 395:347–353.
- Weber, T., B.V. Zemelman, J.A. McNew, B. Westermann, M. Gmachl, F. Parlati, T.H. Sollner, and J.E. Rothman. 1998. SNAREpins: minimal machinery for membrane fusion. *Cell*. 92:759–772.
- Weimbs, T., K. Mostov, S.H. Low, and K. Hofmann. 1998. A model for structural similarity between different SNARE complexes based on sequence relationships. *Trends Cell Biol.* 8:260–262.
- Winzler, E.A., D.D. Shoemaker, A. Astromoff, H. Liang, K. Anderson, B. Andre, R. Bangham, R. Benito, J.D. Boeke, H. Bussey, et al. 1999. Functional characterization of the *S. cerevisiae* genome by gene deletion and parallel analysis. *Science*. 285:901–906.
- Wolfe, K.H., and D.C. Shields. 1997. Molecular evidence for an ancient duplication of the entire yeast genome. *Nature*. 387:708–713.
- Yang, B., L. Gonzalez Jr., R. Prekeris, M. Steegmaier, R.J. Advani, and R.H. Scheller. 1999. SNARE interactions are not selective. Implications for membrane fusion specificity. *J. Biol. Chem.* 274:5649–5653.